



# final report

Project code: A.TEC.0047  
Prepared by: Q. Zou, S. Leath and D. Graham  
AgResearch  
Date submitted: April 2008

PUBLISHED BY  
Meat & Livestock Australia Limited  
Locked Bag 991  
NORTH SYDNEY NSW 2059

## **Model based interpretation of sensors and measurement for bone location and cut line prediction**

Meat & Livestock Australia acknowledges the matching funds provided by the Australian Government and contributions from the Australian Meat Processor Corporation to support the research and development detailed in this publication.

This publication is published by Meat & Livestock Australia Limited ABN 39 081 678 364 (MLA). Care is taken to ensure the accuracy of the information contained in this publication. However MLA cannot accept responsibility for the accuracy or completeness of the information or opinions contained in the publication. You should make your own enquiries before making decisions concerning your interests. Reproduction in whole or in part of this publication is prohibited without prior written consent of MLA.

## **Executive summary**

This project has demonstrated the ability to use sparse data from a carcass sensor (in this instance X-ray images) to deform a computer model such that key carcass attributes (cutting locations) could be identified (including extrapolating to locations not within the X-ray images) and outputted to a Plant System.

The project used data from the MLA funded “Automated Cutting of Lamb Carcasses Using X-ray Imaging” project implemented by Scott Automation.

The image processor and Model Deformation algorithms showed excellent correlation between the software outputs and manually assessed data (maximum error of prediction <6mm). However, the image processing module failed to consistently find a key Landmark Position for the rump region of the carcass. When this Landmark Position was manually located and inputted, the software was able to deform the carcass model to represent the “actual” carcass and output accurate results for the cutting locations (including locations not within the X-ray images)

Excellent progress has been made on this project and the project goals are still considered to be attainable; however this project has run out of time and now needs to be reassessed

## Contents

		Page
1	Introduction.....	4
1.1	Application for demonstration .....	4
1.2	Objectives .....	4
2	Image processing algorithms.....	6
2.1	Purposes of image processing .....	6
2.2	Image processing algorithms .....	6
3	Model customisation .....	7
3.1	Model customisation approach.....	7
3.2	Model customisation method.....	8
3.3	Customised Model Output Data.....	8
4	Results.....	9
5	Conclusion .....	10
6	Reference .....	11

# **1 Introduction**

This project leveraged AgResearch's existing anatomic carcass models and model customisation techniques to create a model-based sensor and measurement interpretation module. These techniques use spatial data acquired from suitable sensing or measurement systems such as 2D colour images, 3D surface data from laser scanning, ultrasonic images, etc. The interpretation module processes spatial information to extract a set of landmark points of various key locations of the carcass. The Landmark Points are used to deform the generic carcass model to create a customised model for the carcass from which the measurements required for the automation application are obtained.

## **1.1 Application for demonstration**

---

The functions of the model-based interpretation module were applied to an MLA funded project known as "Automated Cutting of Lamb Carcasses Using X-ray Imaging" implemented by Scott Automation. This application has been identified as a key application where measurement accuracy is a key technological hurdle.

In this application, the coordinates of the cutting positions are required for automated cutting of a lamb carcass. It is difficult to accurately locate all cutting positions from the x-ray image of the carcass as some key anatomic points, such as the location of first rib, may be obscured. The anatomic model-based method was used to identify the obscured locations, and to validate the coordinates of the cutting positions extracted from the x-ray images (Figure 1).

## **1.2 Objectives**

---

The objectives of this project were to:

Develop and implement the algorithms for processing the x-ray images of lamb carcasses to extract the landmark points.

Develop and implement the algorithms for customising the generic lamb models using the extracted landmark points.

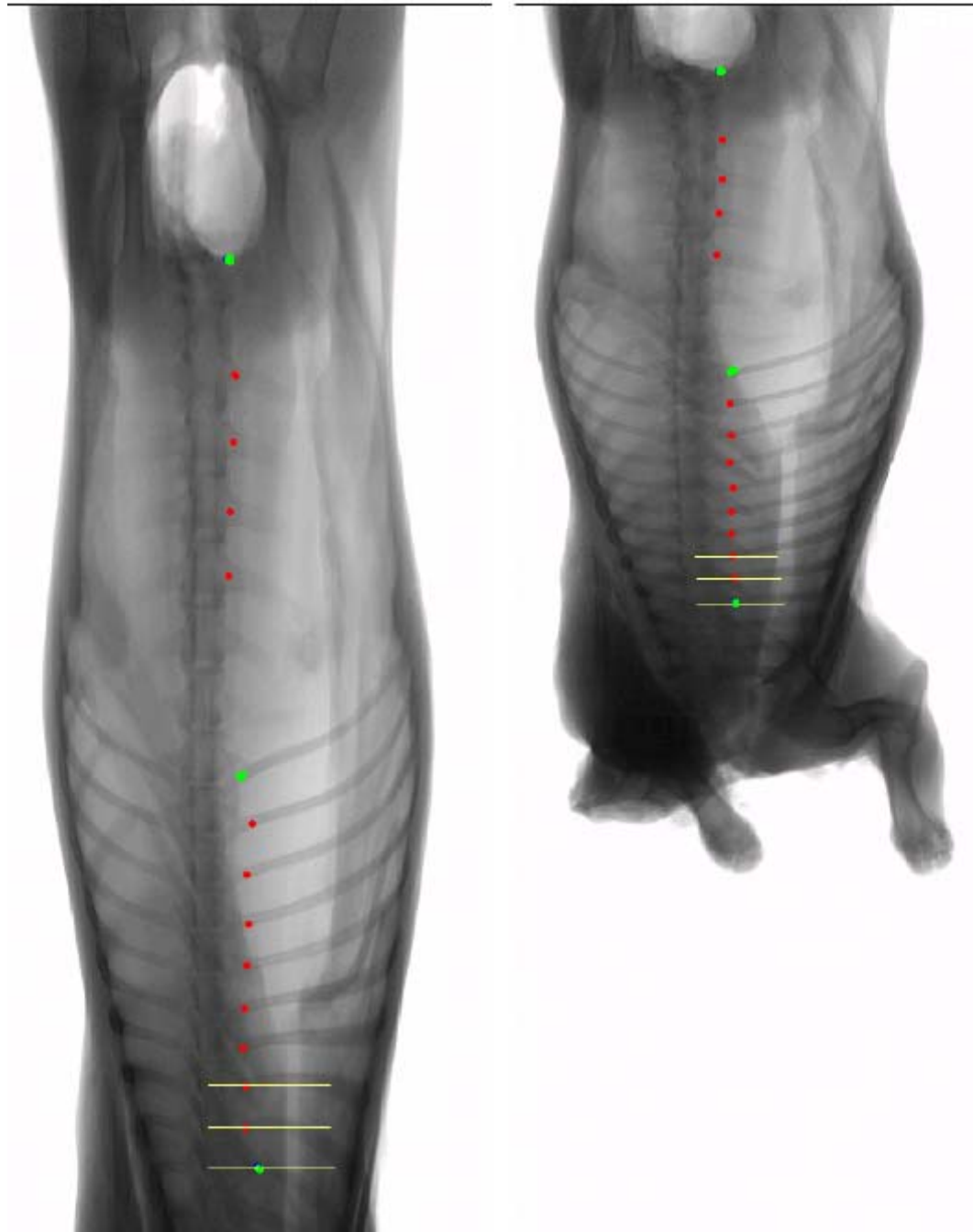


**Figure 1 X-ray images of lamb carcase.**

Green dots are the key landmark points which are always needed for model customisation. Red dots are the landmark points that will be used if they can be retrieved. Yellow lines are cutting position 4<sup>th</sup>, 5<sup>th</sup>, and 6<sup>th</sup> ribs.

## 2 Image processing algorithms

### 2.1 Purposes of image processing

---

In the “Automated Cutting of Lamb Carcasses Using X-ray Imaging” project, two X-ray images (from slightly different angles) are obtained, thus allowing stereoscopic (3D) data for each carcass to be developed.

In the PRTEC.047 project, these x-ray images were processed to extract the following information.

1. Spine position.
2. As many ribs as possible.
3. As many lumbar vertebrae as possible.

The above information was used to extract landmark points for the model customisation.

### 2.2 Image processing algorithms

---

Both x-ray images were processed with the following algorithms, although with slightly different processing parameters:

1. Extract the spine line on each of the two x-ray images
  - Specify narrow long regions of spine in the middle of x-ray images.
  - Improve the contrast of the spine lines by top-hat morphological operations using horizontal structure elements.
  - Link the break sections of the spine lines by open morphological operations using small vertical structure elements.
  - Identify the spine lines as the longest connected region.
  - Remove additional noisy regions attached to the spine line.
  - Extend the spine lines to the whole carcasses.
2. Identify right top ribs on the two x-ray images (10<sup>th</sup> -13<sup>th</sup> ribs and possible 14<sup>th</sup> ribs).
  - Improve the contrast of top ribs by top-hat morphological operations using relatively long vertical structure element.
  - Link the break sections of ribs by open morphological operations.
  - Remove small noisy regions between ribs.
  - Identify the top 4 or 5 ribs as the long horizontal connected regions.
  - Identify the middle line of the ribs by thinning and hit-and-miss operations.
  - Find the distance ranges of rib middle lines, and check if there are falsely identified or missing ribs according the distance ranges.
3. Identify right bottom ribs on two x-ray images (1<sup>st</sup>–9<sup>th</sup> rib)
  - Specify the region of interest for the right bottom rib (the region below top rib and on the right of spine lines)

- Improve the contrast of bottom rib by top-hat morphological operations using relatively small vertical structure element.
  - Link the break sections of rib by open morphological operations
  - Remove small noisy regions between ribs.
  - Identify the bottom ribs as the horizontal connected region.
  - Identify the middle lines of the ribs by thinning and hit-and-miss operations.
  - Find the distance ranges of rib middle lines, and check if there are falsely identified or missing ribs according the distance ranges.
4. Identify lumber vertebrae on two x-ray images
- Specify the region interest for the lumber vertebrae (the narrow region along right side of spine line and above the top ribs).
  - Improve the contrast of lumber vertebrae by top-hat morphological operations using relatively long vertical structure element.
  - Link the break sections of lumber vertebrae by open morphological operations.
  - Remove small noisy regions between lumber vertebrae.
  - Identify the top lumber vertebrae as the horizontal connected regions.
  - Identify the middle lines of the lumber vertebrae by thinning and hit-and-miss operations.
  - Find the distance ranges of vertebrae middle lines, and check if there are falsely identified or missing bones according to the distance ranges.
5. Check if the top rib is 14<sup>th</sup> rib on the x-ray image with the bigger carcass projection
- Identify the end of tail bone.
  - Decide if the top rib is 14<sup>th</sup> rib by counting the number of identified lumber vertebrae or comparing the distance from the end of tail bone to the top rib with the distance between lumber vertebrae.

## 3 Model customisation

### 3.1 Model customisation approach

---

Model customisation was implemented as follows:

- Identify a set of landmark points on the carcass model
- Identify the cutting positions on the carcass model
- Extract the corresponding landmark points at the x-ray images of an individual carcass, and calculate 3D coordinates of landmark points for the carcass
- Deform the deformation lattice using the landmark points on the individual carcass as the target points and the landmark points on carcass model as original the points (see section 3.2)

- Calculate the cutting positions using the deformation lattice

For current application, only the heights of cutting positions are needed for locating cutting lines. Therefore model customisation is only performed along the height and depth directions while the model coordinates at width direction remain unchanged.

We selected the landmark points at the ends of rib and lumber vertebrae lines close to carcase spines as shown in Figure 1 (red and green dots), as the positions of these points are consistent for most of the carcasses. Due to variation on x-ray image quality, not all rib and lumber vertebrae positions can be retrieved with image processing and the landmark points are not always the same. However three key landmark points (end of 4<sup>th</sup> rib, end of 13<sup>th</sup> rib, and end of vertebrae, green dots in Figure 1) are always needed for performing full scale model customisation. In general model customisation uses all available landmark points.

### **3.2 Model customisation method**

---

The model customisation method was implemented in a more general 3D framework, which can be easily used for 2D customisation by simple setting the 3D dimension as constant.

Free-form deformation (FFD) is used to customise the generic anatomic models. The deformation tool in FFD is a parallel piped lattice or volume (deformation lattice), in which the object to be deformed is embedded. To deform the embedded object the user deforms the lattice by moving its control points (Sederberg & Parry, 1986). This technique has been extended to include lattices of non-parallelepiped or arbitrary topology (Coquillart 1990; MacCracken and Joy 1996), and B-splines or NURBS volumes (Griessmair and Purgathofer 1989; Lamousin and Waggenspack 1994). Hu et al. (2001) developed a method for direct manipulation of free-form deformation by minimising FFD lattice deformation while satisfying the constraints imposed by landmark points.

Instead of using complex deformation techniques, we used B-spline volume as deformation lattice, and Bezier volume was included as a special case of B-spline lattice. The complex geometries of anatomic models can be easily handled with fine lattices due to fast growing computation capacity of PCs.

### **3.3 Customised Model Output Data**

---

The target cutting locations were identified within the deformed model and outputted to a data file (simulating a Plant IT System). The outputs selected were;

- Forequarter separation co-ordinates, defined as 4<sup>th</sup>, 5<sup>th</sup> and 6<sup>th</sup> rib.
- Middle Separation (Chump-off Middle) co-ordinates, defined as the lowest points on the aitch bone.
- Middle Separation (Scallop Cut Middle) co-ordinates, defined as the top vertebrae.
- Middle Separation (Chump-on Middle) co-ordinates, defined as the bottom of the socket.
- Points on the aitch bone for removal of the legs

Note: Data for the Locations 4 and 5 do not appear in the X-ray images

A dataset independent from the dataset (images) used in the image processor is required to validate the image processor. Such a dataset might, for example, comprise lineal measurements to locations on the carcase taken with callipers and rulers, or photographs of the carcase against a grid of known dimensions. Such an independent dataset was not received for the images



obtained from Scott Technologies. Therefore a quasi-independent validation dataset was created by manually assessing the output locations of the 4<sup>th</sup> and 5<sup>th</sup> ribs in the X-ray images, extracting their heights (using the angle of the X-rays incident on the receiver) and entering their spatial data into a spreadsheet.

The “Plant” data file was opened, compared to the validation file and the Standard Error of Prediction determined.

## 4 Results

75 image sets were used to test and validate the image processor and model deformation algorithms.

The images were processed through the image processing software. The algorithms were able to define Landmark Positions around the ribs; however they were unable to find a consistently suitable Landmark Position around the aitch bone/vertebrae/rump region (top green dot in Figure 1). The angle of projection in this region meant that easily identified locations were not available in every image (such as hip balls) or were obscured by thick portions of the legs (e.g. vertebrae/aitch bone). Without a Rump Region Landmark Position the model customisation software was unable to deform the model with sufficient resolution that the output results were accurate enough to be used in cutting operations.

In order to progress the project to the stage of testing the actual model deformation software, a rump region Landmark Position was defined to be the junction of the top vertebrae and the aitch bone. This position was manually located in the images and entered as a variable in the deformation software and the 75 images processed. Figure 2 and Table 1 compare the heights of the 5<sup>th</sup> and 6<sup>th</sup> ribs obtained from model customisation with the validation data that are the height values calculated from manually located positions on x-ray images (top two yellow lines in Figure 1).

Note: Automating the derivation and inputting the Rump Region Landmark Position will need to be completed.

Table 1 **Difference between manual validation set and deformed model**

	5th rib	6 <sup>th</sup> rib
Average Difference (mm)	-1.1367	-1.162
Standard Error of Prediction	2.014	1.4245
Maximum Difference (+/-)	5.037	5.255

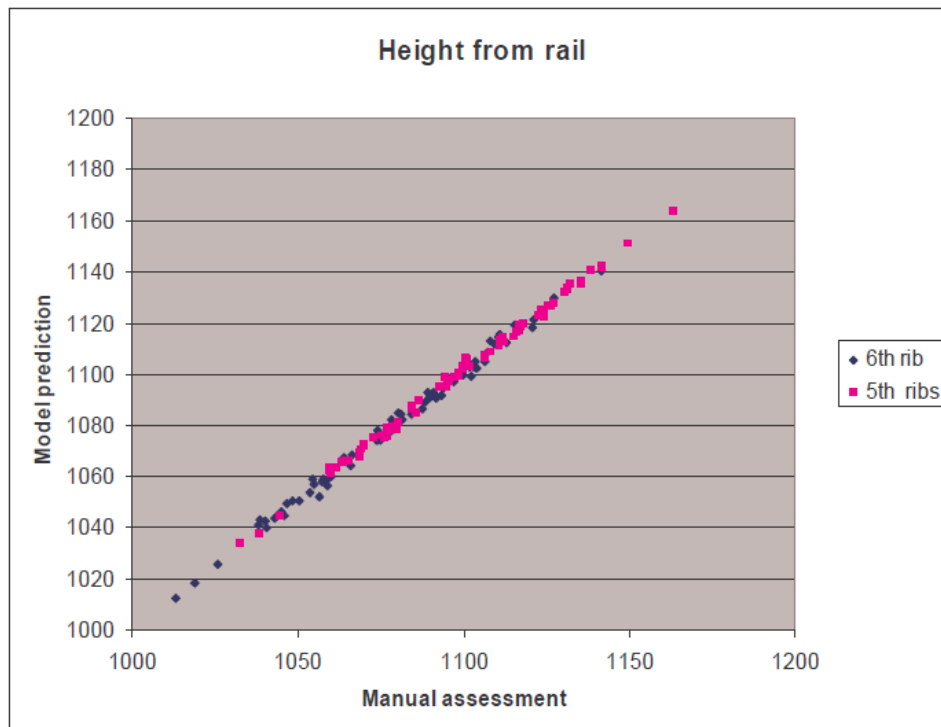


**Figure 2 Comparison between model prediction and manual assessment.**

Figure 2 shows the linearity of the output of the deformed model against the manually derived validation data.

## 5 Conclusion

The image processing and deformation modules appear to work well with excellent correlations to the quasi-independent validation dataset. It would be wise to run a trial using a fully independent datasets i.e. images from carcasses that have been measured using, for example, rulers.

The software is not yet fully automated and currently requires a Landmark Position within the rump region to be manually identified and inputted using a prompt box. Time has not permitted the development of an algorithm to reliably define and find such a point. However this is seen to be an achievable goal.

Although achieving the overall project goals is still seen as achievable, this project has run out of time and needs to be closed and reassessed.

In essence, the image processor and model deformation algorithms:

1. Failed to consistently find a key Landmark Position for the rump region of the carcass.
2. Were able to deform the carcass model to represent the “actual” carcass with very good accuracy.
3. Were able to output accurate results for the 4<sup>th</sup>, 5<sup>th</sup> and 6<sup>th</sup> rib cutting locations.

## 6 Reference

- Borrel P, Bechmann D (1991) Deformation of N-dimensional objects. *Int J Comput Geom Appl* 1(4): 137–155
- Coquillard S, Jancène P (1991) Animated free-form deformation: an interactive animation technique. *Comput Graph* 25(4): 23–26
- Coquillard S (1990) Extended free-form deformation: a sculpturing tool for 3D geometric modeling. *Comput Graph* 24(4): 187–193
- Griessmair J, Purgathofer W (1989) Deformation of solids with trivariate B-spline. In: Hansmann W, Hopgood FRA, Strasser W (eds) *Proc. Eurographics '89*. Elsevier, North- Holland, pp 137–148
- Hsu WM, Hughes JF, Kaufman H (1992) Direct manipulation of free-form deformation. *Comput Graph* 26(2): 177–184
- Hu SM, Zhang H, Tai CL, Sun JG. (2001) Direct manipulation of FFD: efficient explicit solutions and decomposable multiple point constraints. *Visual Computer* 17: 370-379
- Lamoussin HJ, Waggenspack WN (1994) NURBS-based free-form deformations. *IEEE Comput Graph Appl* 14(6): 59–65
- Lazarus F, Coquillard S, Jancène P (1994) Axial deformation: an intuitive technique. *Comput Aided Des* 26(8): 607–613
- MacCracken R, Joy K (1996) Free-form deformation with lattices of arbitrary topology. *Comput Graph* 30(4): 181–189
- Schumaker LL (1980) *Spline functions: basic theory*. Wiley, New York
- Sederberg TW, Parry SR (1986) Free-form fundamentals of solid geometry. *Comput Graph* 20(4): 151–160
- Wahba G (1990) *Spline Models for Observational Data*. Society for Industrial and Applied Mathematics.